Separation Science and Technology
Publication details, including instructions for authors and subscription information:
http://www.informaworld.com/smpp/title~content=t713708471

Characterization of Steric Field-Flow Fractionation Using Particles to 100 µm Diameter

Richard E. Peterson II[a]; Marcus N. Myers[a]; J. Calvin Giddings[a]
[a] UNIVERSITY OF UTAH DEPARTMENT OF CHEMISTRY SALT LAKE CITY, UTAH

To cite this Article Peterson II, Richard E. , Myers, Marcus N. and Giddings, J. Calvin(1984) 'Characterization of Steric Field-Flow Fractionation Using Particles to 100 µm Diameter', Separation Science and Technology, 19: 4, 307 — 319
To link to this Article: DOI: 10.1080/01496398408068585
URL: http://dx.doi.org/10.1080/01496398408068585

SEPARATION SCIENCE AND TECHNOLOGY, 19(4 & 5), pp. 307-319, 1984

Characterization of Steric Field-Flow Fractionation Using Particles to 100 μm Diameter

RICHARD E. PETERSON II, MARCUS N. MYERS, and J. CALVIN GIDDINGS

UNIVERSITY OF UTAH
DEPARTMENT OF CHEMISTRY
SALT LAKE CITY, UTAH 84112

Abstract

Steric field-flow fractionation has been applied to a larger range of particle sizes than heretofore studied, thus expanding the upper diameter limit to approximately 100 μm. The large size range investigated (6–100 μm), combined with velocity-dependent studies, provided the parameters for two simple empirical retention equations. The implication of these equations to selectivity and plate height were investigated theoretically. The experimental results, combined with the theory, showed that the diameter-based selectivity was less than unity and decreased somewhat with increasing velocity. Calculated polydispersity contributions appeared to constitute a major part of peak broadening, but observed plate heights increased with flow velocity whereas the polydispersity contribution was predicted to decrease with velocity. The theoretical and practical implications of the results are summarized.

INTRODUCTION

Steric field-flow fractionation, or steric FFF, is that limiting form of FFF in which particle position in the cross section of the flow channel, and thus particle retention, is controlled by the steric effects of finite particle diameter rather than by a diffusion process (*1*). This limit is generally realized for any large particle for which the "field" force F of FFF is relatively high. F must be of such a magnitude that $Fa > kT$, where a is particle radius, k is the Boltzmann constant, and T is the temperature. Steric conditions generally begin to come into dominance at about 1 μm particle diameter (*2*). It was

 0149-6395/84/1904-0307$3.50/0

originally anticipated that steric FFF would be effective at least over the particle diameter range 1–100 μm, but the largest particles so far fractionated have been 32 μm (*1*).

One object of this work is to extend the upper diameter limit of experimental FFF and to examine any problems attendant to that expansion. Another object is to better characterize retention, zone broadening, and selectivity characteristics in steric FFF.

The retention ratio R, which is the ratio of channel void volume V° to retention volume V_r, can be expressed by

$$R = 6\gamma a/w = 3\gamma d/w \tag{1}$$

in which the particle dimensions are expressed either by radius a or diameter d, and channel width is expressed by w. For the ideal case, in which the particle is carried along the channel wall with the velocity of the flow stream at a distance of one particle radius away from the wall, we have $\gamma = 1$. Departures of the factor γ from unity, then, are a measure of departures from this ideal situation.

Unfortunately, parameter γ has not been very well characterized. Its departure from unity reflects rather complicated hydrodynamic phenomena, making theoretical treatment difficult. Prior experiments in our laboratory have been accompanied by an inexplicably high lack of repeatability and reproducibility.

The extension of the present study to large particles (up to 100 μm) provides an opportunity to study a wide range of particle diameters and thus to look at particle diameter effects in steric FFF. In addition, we have elected to look at the effect of flow velocity on retention. From previous experimental work we have recognized that R always increases with velocity (*3*), which is a situation unlike that for normal FFF where R is relatively velocity-independent.

THEORY

Theoretical considerations indicate that R, and therefore γ, must approach zero as flow velocity approaches zero. An unpublished heuristic theory developed in our laboratory suggests that R and γ increase with the ½ power of velocity, which at least approaches the desired limit of $\gamma = 0$ for zero velocity. For purposes of consistency with this limit, we will look first at an equation which satisfies this zero intercept condition. In particular, we will begin with the simplest possible assumption consistent with that limit, namely that γ increases with some power of velocity. The particle diameter

dependence will be formulated similarly. (The heuristic treatment suggests that γ depends on diameter d to the minus ½ power.) Thus we will examine the applicability of the equation

$$\gamma = C\langle v\rangle^{\alpha} d^{\beta} \tag{2}$$

where C is a constant, $\langle v\rangle$ is the average flow velocity in the channel, and the exponents α and β are to be determined from empirical evidence.

Second, we will examine an equation which is consistent with the empirical results presented later in this paper. In particular, our equation will show a linear relationship between γ and $\langle v\rangle$, but both the intercept and slope will depend on d. When expressed mathematically, we have

$$\gamma = K_1 d^{\theta 1} + K_2 d^{\theta 2}\langle v\rangle \tag{3}$$

where K_1, K_2, θ_1, and θ_2 are constants to be determined empirically.

The values of the empirical constants in the above two γ equations have specific implications with respect to selectivity and plate height, and many general implications regarding system optimization. The reasons are given below.

One of the implications of a dependence of γ on d is that selectivity will be directly affected. The diameter-based selectivity of a fractionation method is simply (*2*)

$$S_d = \frac{d \log V_r}{d \log d} = \frac{d \log R}{d \log d} \tag{4}$$

The substitution of Eq. (2) into Eq. (1) and the latter into Eq. (4) yields

$$S_d = 1 + \beta \tag{5}$$

Thus, if $\beta > 1$, S_d will be larger than the unit value usually assumed, and if $\beta < 1$, S_d will be less than unity.

Following the same procedure with Eq. (3) in place of Eq. (2) leads to

$$S_d = \frac{K_1(1 + \theta_1)d^{\theta 1} + K_2(1 + \theta_2)d^{\theta 2}\langle v\rangle}{K_1 d^{\theta 1} + K_2 d^{\theta 2}\langle v\rangle} \tag{6}$$

This expression shows S_d to approach the following limit as flow velocity approaches zero:

$$\lim_{\langle v \rangle \to 0} S_d = 1 + \theta_1 \tag{7}$$

Similarly, for very high velocities, S_d approaches the limiting value

$$\lim_{\langle v \rangle \to \infty} S_d = 1 + \theta_2 \tag{8}$$

Thus, whether the optimum velocity insofar as S_d is concerned is high or low depends on the relative values of θ_1 and θ_2. For high separation speed, of course, high flow rates are preferred.

A feature of steric FFF besides retention which has been poorly characterized is zone broadening. The experimental study of zone broadening has been complicated by the lack of monodisperse samples. The theoretical study has been complicated by uncertainty concerning the form of the polydispersity contribution to zone broadening and the lack of a well-defined nonequilibrium term (or any other well-characterized contribution) to the zone spreading process. For spherical beads in a geometrically perfect channel, there should be only minor sources of zone broadening aside from the polydispersity effect.

The polydispersity effect can be characterized, providing we have a retention equation, using methods developed previously (*4, 5*). Application of those methods to Eq. (1) with γ expressed by Eq. (2) gives for the polydispersity contribution to plate height

$$H_p = (\beta + 1)^2 L(\sigma_d/d)^2 \tag{9}$$

where L is channel length and σ_d is the standard deviation in particle diameter, a term that represents sample polydispersity. Application to the case in which γ is given by Eq. (3) gives

$$H_p = \left[\frac{K_1(1 + \theta_1)d^{\theta_1} + K_2(1 + \theta_2)d^{\theta_2}\langle v \rangle}{K_1 d^{\theta_1} + K_2 d^{\theta_2}\langle v \rangle} \right]^2 L \left(\frac{\sigma_d}{d} \right)^2 \tag{10}$$

EXPERIMENTAL

Two channels were used, both of identical cross sections, 2 cm wide by 0.5 mm thick. The channels were cut from 0.020 in. (508 μm) thick Teflon sheets into the length and shape desired. One channel, labeled Channel I, was 15.4 cm long, and the other, Channel II, was 85.6 cm long measured

from inlet to outlet. There were two slightly different versions of Channel I, labeled Ia and Ib, respectively, which had void volumes of 1.57 and 1.50 mL, respectively. The small difference was found upon reassembling the system after it was opened for cleaning. Channel II was found to have a void volume of 8.84 mL. The void volumes were determined by measuring the retention volume of the nonretained solute, sodium benzoate. The channel ends were triangular and converged at 45° onto the inlet and outlet ports.

The Teflon spacer with the channel area removed was sandwiched between two glass plates, the bottom one covered with 0.003 in. (77 μm) Teflon tape. The glass plates, in turn, were clamped between Plexiglas blocks with holes drilled for nuts and bolts. The bolts for Channel I were torqued to 35 in.-lb and for Channel II to 25 in.-lb. The detector was Altex (Berkeley, California) Model 153 UV detector operated at 254 nm. Pumps used were a Gilson (Middleton, Wisconsin) Minipuls 2 peristaltic pump for low flow rates and a Crane (Warrington, Pennsylvania) Chem/Meter series 20 for high flow rates (up to 10 mL/min). Bellows-type pulse dampeners were needed for both pumps. For later work we employed a Kontron (London, UK) Analytic LC Pump 10, which worked well without a pulse damper. The recorder used was an Omniscribe recorder from Houston Instruments (Austin, Texas).

The samples were "monodisperse" polystyrene latex spheres of reported diameter 90.7 μm (± 17.7 μm), 25.7 μm (± 10 μm), 5.7 μm (± 1.5 μm), and 6.0 μm (± 0.5 μm) from Polysciences, Inc. (Warrington, Pennsylvania), and 99.3 μm (± 5.0%), 60.9 μm (± 5.9%), 25.3 μm (± 9.5%), and 11.3 μm (± 8.0%) from Duke Scientific (Palo Alto, California). Particle density was 1.05 g/mL. Between 10 and 40 μL samples of the suspensions were injected by syringe.

The carrier liquid was distilled, degassed, deionized H_2O with 0.1% FL-70 detergent (Batch 703765, Fisher Scientific Co., Fair Lawn, New Jersey). All runs were carried out at room temperature, 25 ± 1°C.

Volumetric flow rate was varied between 0.6 and 10 mL/min, giving a linear velocity range of 0.1 to 1.65 cm/s. Generally, 4 or 5 runs were made per sample at each flow rate. Following sample injection, the flow was stopped for a period adequate to allow the particles to relax to the lower wall. The minimum relaxation time was calculated from the Stokes-Einstein equation. This stop-flow procedure was used for all but the 99.3 μm beads, which settled so rapidly that stop flow was not considered necessary.

After each run the system was flushed with ethanol via a large syringe to remove any beads or pieces of septum left in the channel. Weekly, the system was filled with a solution of Hematall Detergent (Fisher Scientific Co.) and left overnight to prevent bacterial or algal growth.

Retention data were acquired by measuring the position of the peak maximum and expressing this in terms of retention volume V_r. Plate height values were calculated from the width at half height.

RESULTS AND DISCUSSION

Initial work was done with Channel Ia. This channel provided reproducible retention (average standard deviation in R about 4%) for the nominal 90.7 μm beads. Since the 90.7-μm bead sample is somewhat polydisperse (90.7 $\pm$ 17.7 μm as reported, but more widely dispersed based on our microscopic observation), a substantial fraction of the beads are actually over 100 μm, thus extending the upper limit of practical steric FFF to approximately 100 μm particle diameter.

With regards to fractionation, channel Ia achieved the separation of the 90.7, 25.7, and 5.7 μm Polysciences beads in as little as 9 min total run time, including 3 min stop-flow time for relaxation, at a flow rate of 9.58 mL/min. Resolution was good. Similar results are shown in Fig. 1 for a flow rate of 1.77 mL/min.

Subsequent work, using Column Ib, was done on the 99.3 μm beads, again providing results extending into the 100-μm range. These particles were subjected to retention studies only; they provided significant levels of retention with reproducible R values which depend on flow velocity. The observed values of R were 0.290 $\pm$ 0.005, 0.302 $\pm$ 0.005, 0.322 $\pm$ 0.004, 0.357 $\pm$ 0.005, and 0.427 $\pm$ 0.011 for the linear velocity $\langle v \rangle$ values of 0.500, 0.667, 0.833, 1.00, and 1.65 cm/s, respectively. The increase in R(or γ) with $\langle v \rangle$ is typical, as we shall see below.

Considerable difficulty was realized in applying Column II to the larger beads (60.9 μm and larger). The problem of the weaker intrinsic detector signal for a given mass of larger beads appeared to be compounded by sample loss in the column. Microscopic observation of a test channel showed a considerable number of beads sticking to the surface.

Figures 2 and 3 show the experimental γ values plotted as a function of $\langle v \rangle$ for Columns Ia and II, respectively. (The results for Column Ib are much like those for Ia, but are more limited and are not shown in graphical form.) For each nominal bead size we have shown two lines which represent the best fit of the data to Eqs. (2) (curved line) and (3) (straight line), respectively. The parameters corresponding to the best-fit lines are summarized in Table 1. These parameters were obtained individually for Columns Ia, Ib, and II using Simplex minimization as developed by Nelder and Mead (*6*) and implemented by O'Neill (*7*).

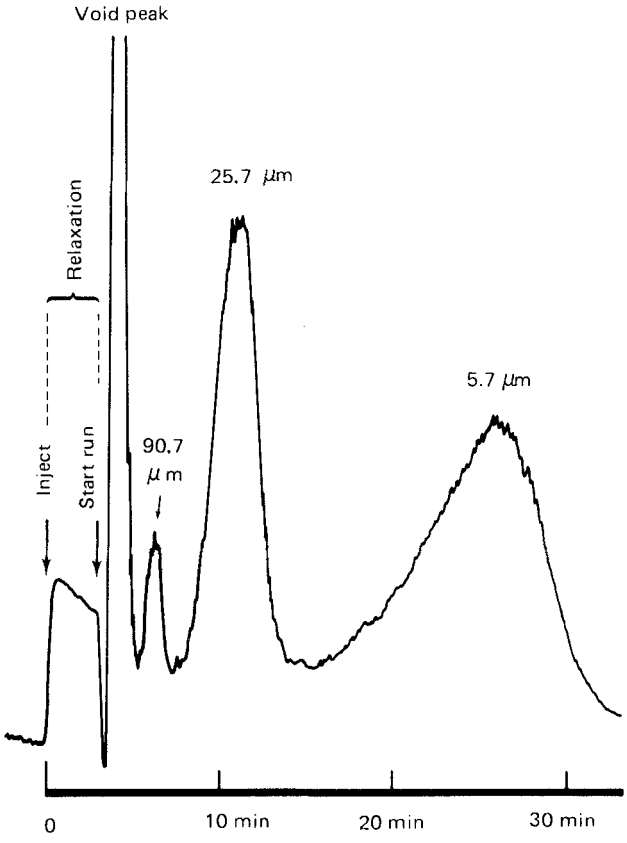

FIG. 1. Separation of three indicated bead sizes using steric FFF, Column Ia.

Figures 2 and 3 show unequivocally that factor γ at any given flow velocity decreases with increasing particle diameter d. This observation is reflected quantitatively in Table 1 by the generally negative values of the exponents (β, θ_1, θ_2) of d resulting from the fit of data to Eqs. (2) and (3). Unfortunately, this trend leads to a decrease in selectivity S_d below unity, as shown by Eqs. (5)–(8). It also appears that θ_2 is generally a larger negative number than θ_1, leading to a decrease in S_d with increasing $\langle v \rangle$ as shown by limiting Eqs. (7) and (8).

Figures 2 and 3 also show that Eq. (3) fits the data somewhat better than Eq. (2). This observation is confirmed by Table 2 which shows the average deviation of the data from the best-fit lines provided by Eqs. (2) and (3),

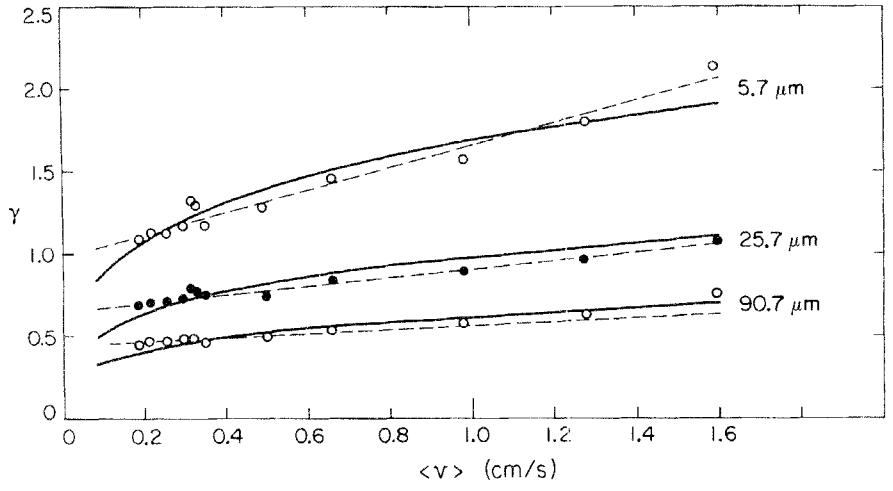

FIG. 2. Experimental γ data for Column Ia and best fit to Eq. (2) (curved lines) and Eq. (3) (straight lines).

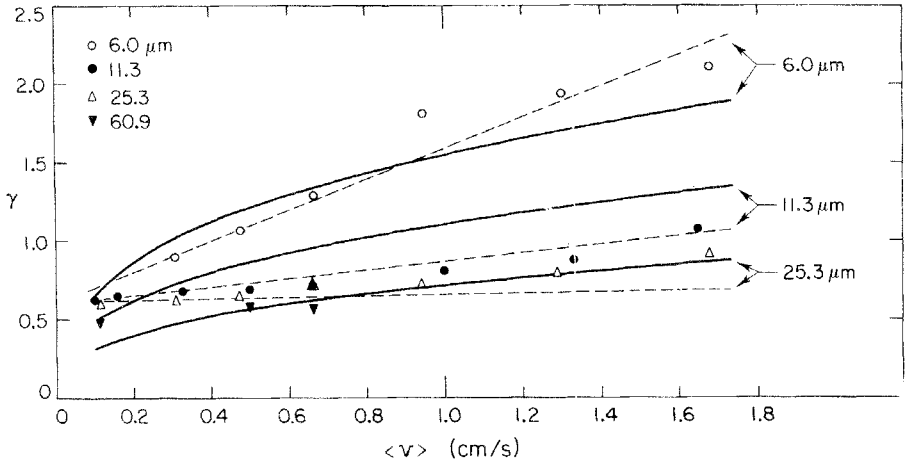

FIG. 3. Experimental γ data for Column II and best fit to Eq. (2) (curved lines) and Eq. (3) (straight lines). Curves are not shown for limited 60.9 μm data.

respectively. (The average value of the standard deviation of γ measured under fixed conditions is also shown for comparison.) Equation (3), of course, has more adjustable parameters, four as opposed to three for Eq. (2). The real difficulty with Eq. (2) appears to be that of having a form somewhat too simple to describe the transition of γ to zero as $\langle v \rangle$ approaches zero. Unfortunately, this transition would be extremely difficult to observe experimentally because of the slow speed of the $\langle v \rangle \rightarrow 0$ experiments and the tendency of beads to adhere to the surface at low $\langle v \rangle$ values. Clearly, more theoretical work is required in this area because of the experimental difficulties.

Table 1 shows that the parameters for Columns Ia, Ib, and II all follow the same general trends, although individual variations are evident. The parameters depending primarily on d (especially the exponents β, θ_1, and θ_2) are perhaps most reliably given by Column Ia because of the larger (15–fold) particle size range examined with this column. The parameters derived from Eq. (2) are the most definitive in showing the overall dependence of γ on both $\langle v \rangle$ and $\langle d \rangle$: the dependence on $\langle v \rangle$ is approximately expressed by the power $\alpha = 0.3$ while the dependence on d—somewhat more erratic—averages to the power $\beta = -0.4$. The latter suggests that a typical selectivity, from Eq. (5), would be approximately $S_d = 0.6$.

Unfortunately, the zone spreading (plate height) data are far less consistent than the retention data discussed above. Whereas the standard deviation in γ, shown in Table 2, suggests a random error of 2–4%, the random error in H was often an order of magnitude greater. Therefore, the data do not permit more than the expression of approximate H values and the

TABLE 1

Parameters in Retention Eqs. (2) and (3) Resulting from the Best Fit to the Experimental Data from Each Column. These Parameters Are Applicable with d Expressed in μm and $\langle v \rangle$ in cm/s. Results for Column Ia Based on 90.7, 25.7, and 5.7 μm Beads; Ib Based on 99.3 and 60.9 μm Beads; II Based on 60.9, 25.3, 11.3, and 60 μm Beads

Equation	Parameter	Column Ia	Column Ib	Column II
2	C	3.183	1.941	4.052
2	α	0.273	0.296	0.359
2	β	−0.366	−0.254	−0.539
3	K_1	1.614	0.404	0.626
3	K_2	2.027	2.061	38.660
3	θ_1	−0.289	−0.005	0.011
3	θ_2	−0.622	−0.496	−2.049

TABLE 2
Comparison of the Average Deviation of the Retention Data, Expressed as γ, from the Lines of Best Fit for Eqs. (2) and (3), Respectively. The average of All Standard Deviation Values in γ for Each Column are Shown for Comparison

Equation	Quantity	Column Ia	Column Ib	Column II
2	Average deviation from best fit	0.066	0.060	0.182
3	Average deviation from best fit	0.038	0.041	0.093
—	Standard deviation of experimental data	0.029	0.035	0.017

overall trend of H with changes in flow velocity $\langle v \rangle$. These results are obtained by fitting the data for each bead size to a linear expression

$$H = H_0 + (dH/d\langle v \rangle)\langle v \rangle \tag{11}$$

The results of this analysis are shown in Table 3. Also shown in the table are H_p values calculated from Eq. (9) using the (σ_d/d) values given by the supplier and noted earlier, and the β values shown in Table 1. For the most direct possible comparison with H_p, we have compiled an overall experimental value for plate height designated by $\tilde{\tilde{H}}$(obs), defined as the H value calculated from Eq. (11) using the best-fit intercept and slope parameters of Table 3 and a flow velocity $\langle v \rangle$ midway through the range of experimental $\langle v \rangle$ values. A comparison of $\tilde{\tilde{H}}$(obs) with the calculated polydispersity contribution H_p arises from the last two columns of Table 3. Considering the uncertainties of this comparison (discussed below), the order-of-magnitude agreement of calculated and observed plate heights is quite good, although the latter tend to be larger. The results suggest that polydispersity is a major component of zone spreading.

A more exact identification of the factors contributing to observed plate height will require, first of all, more precise plate height data. Second, a better theoretical model to account for effects (if any) other than polydispersity would be desirable. Third, the magnitude of the sample polydispersity should be determined independently in order to allow for possible errors in the supplier data. Fourth, the dependence of retention on particle diameter d should be determined more exactly because of the effect of this dependence on S_d and thus H_p.

Despite the above uncertainties, the data of Table 3 show some tendencies which are a logical outcome of theory, assuming that H_p is a major factor. For example, H_p values for Column Ib are predicted to be considerably

smaller than those for Column II because of the shorter column length. This prediction is generally consistent with the data. Furthermore, Column Ia is expected to yield larger values of H_p than Ib because of the greater stated polydispersity of the Ia bead samples. Again, this expectation is realized.

There is one major anomaly which involves the effects of flow velocity. The positive values for slope $dH/d\langle v\rangle$ in all but one case show that there is a strong tendency for H to increase with $\langle v\rangle$. The prediction of Eq. (9) is that H_p will be constant with changes in $\langle v\rangle$, but the greater detail of Eq. (10) suggests that H_p, which is proportional to S_d^2, will shift with increasing $\langle v\rangle$ from a value determined by θ_1 to a value determined by θ_2 (see Eqs. 7 and 8). Since $\theta_1 > \theta_2$, Table 1, H_p should decrease with increasing $\langle v\rangle$. The contrary tendency of the experimental data suggest that some other factor is influencing peak broadening.

CONCLUSIONS

This study is perhaps most useful in establishing, in qualitative and quantitative form, some apparent trends in the dependence of retention, selectivity, and plate height on flow velocity, particle diameter, and sample polydispersity. This is a considerable advance because steric FFF has lacked any clear characterization in this area beyond the qualitative observation that γ tends to increase with flow velocity. However, a previous study from this laboratory has shown the effect of other parameters, particularly particle density and centrifugal field strength, on retention (*3*).

TABLE 3
Plate Height Results for Beads of Different Diameter d Run in Columns Ia, Ib, and II

Column	d (μm)	H_0 (cm)	$dH/d\langle v\rangle$ (cm/s)	$\tilde{\tilde{H}}$(obs) (cm)	H_p(calc) (cm)
Ia	5.7	0.166	0.423	0.547	0.676
	25.7	0.188	0.210	0.377	1.478
	90.7	0.206	0.169	0.358	0.372
Ib	60.9	0.022	0.049	0.066	0.027
	99.3	0.008	0.052	0.064	0.019
II	6.0	0.860	1.440	2.300	0.274
	11.3	−0.156	1.073	0.783	0.253
	25.3	0.390	0.366	0.719	0.365
	60.9	0.470	−0.352	0.333	0.137

This study also raises many important questions that should provide topics for further investigation. For example, plate height H requires better characterization, and the puzzling discrepancy between theory and experiment on changes in H with flow velocity must be resolved. Plate height effects arising outside of polydispersity effects also need investigation.

Sample losses due to surface adhesion, particularly for the larger beads in the longer column, also merit study. One needs to find which surfaces and carrier composition (especially of ionic constituents) best serve to reduce particle–surface and particle–particle interactions.

Eventually, of course, one needs a more universal characterization of steric FFF with respect to all important parameters, not only flow velocity and particle diameter but also particle density, carrier viscosity, channel width, and field strength. This characterization would profit from the establishment of a more complete theoretical base than now exists.

The present work has important practical as well as theoretical implications. The notion that selectivity changes with flow velocity is new, and should be considered in any thorough optimization scheme. The demonstration that there is apparently some plate height term increasing with velocity also bears on optimization, although the velocity-dependence requires better characterization.

We further note that the present analysis should lead to improvements in the characterization of sample polydispersity. The acquisition of polydispersities from peak broadening has been tried before (*8*) based on a simple model. The present work, by developing the form of the polydispersity contribution, is a necessary step in isolating accurately the effects of polydispersity from other effects, which isolation would give direct polydispersity data. We note, for example, that H_p is proportional to column length L, which leads to the suggestion that columns of different lengths can be used to isolate polydispersity values.

Acknowledgment

This work was supported by the Department of Energy Grant No. DE-AC02-79EV10244.

REFERENCES

1. J. C. Giddings and M. N. Myers, *Sep. Sci. Technol., 13*, 637 (1978).
2. M. N. Myers and J. C. Giddings, *Anal. Chem*, 54, 2284 (1982).

3. K. D. Caldwell, T. T. Nguyen, M. N. Myers, and J. C. Giddings, *Sep. Sci. Technol., 14*, 935 (1979).
4. M. E. Hovingh, G. H. Thompson, and J. C. Giddings, *Anal. Chem., 42*, 195 (1970).
5. J. C. Giddings, F. J. F. Yang, and M. N. Myers, *Ibid., 46*, 1917 (1974).
6. J. A. Nelder and R. Mead, *Comput. J., 7*, 308 (1965).
7. R. O'Neill, *J. R. Stat. Soc., Ser. C, 20* (3), 338 (1971) (Algorithm 47).
8. J. C. Giddings, M. N. Myers, K. D. Caldwell, and J. W. Pav, *J. Chromatogr., 185*, 261 (1979).